25X1

C0000899

IMAGE ANALYSIS III (U)

Quarterly Report

by

[redacted] 25X1

[redacted] 25X1

Task 32

Report No. TO-B 68-53

13 September 1968

[redacted] 25X1

[redacted] 25X1

IMAGE ANALYSIS III (U)

Quarterly Report

by

[redacted] 25X1

[redacted] 25X1

Task 32

Report No. TO-B 68-53

13 September 1968

[redacted] 25X1

TABLE OF CONTENTS

LIST OF ILLUSTRATIONS

CHAPTER 1

INTRODUCTION AND SUMMARY

This report describes the work performed during the second quarter of the Image Analysis III program. The studies conducted in this and the previous phases of the program on the effects of coherence on image exploitation instruments are summarized, and the individual instruments of interest are discussed in detail. A nomograph has been devised that enables finding the class of objects for which coherence effects may be expected to occur in any given instrument. This nomograph can also be applied to instruments other than those in current use.

Progress has been made in determining the optimum shaded aperture for the suppression of grain noise in the IDT. The computer program has been improved and the assumptions underlying the procedure have been more rigorously examined.

We have begun experiments to determine if coherent filtering can be used in a microscope to aid in the suppression of grain noise. Initial work along these lines is promising, and the computer program for the IDT can also be applied in this case. Wiener filtering in the IDT and in the microscope appears ideally suited for the recovery of information from photographic records.

We have also conducted experiments to determine if information recovery from photographs can be improved by the introduction of color filters into a microscope. Though some interesting effects can be achieved with non-photographic objects, there is no indication that useful effects can be obtained with photographic records.

Plans have been made for initial experiments to determine if spatial filtering in scanning systems is a useful technique. A standard microdensitometer modified for laser illumination will be used in these experiments.

CHAPTER 2

COHERENCE STUDIES

In the previous phases of this program, extensive studies on the effects of coherence in imaging systems were conducted. These studies included measurements of the intensity distribution in images of various objects for various degrees of coherence of illumination of the object, and measurements of the coherence of the illumination in actual image exploitation instruments. It was found that the presence and extent of coherence effects primarily depend on three factors:

1. Resolution limit of the imaging system
2. Spatial frequency content of the object
3. Spatial coherence of the light illuminating the object.

Other factors such as aberrations in the imaging lens and contrast of the object can also affect the extent to which coherence influences images, but these apply to specific imaging conditions and cannot be included in a general analysis.

CONSTRUCTION AND USE OF NOMOGRAPH

The conditions under which coherence will be a problem in a general imaging system can be found from the nomograph in Figure 1, which was constructed from analysis of the experiments on partially coherent imaging and from coherence measurements. To use this nomograph, first the quantities R and N.A. are determined from the physical characteristics of the system. For the instruments under consideration, these two quantities representing information about the resolution limit and the coherence are easier to determine than other quantities representing the same information. A straight line is then drawn through the R and N.A. columns to intersect the L column, and the spatial frequency for this intersect point is read. For objects containing spatial frequencies less than this intercept frequency, coherence effects will essentially be absent. As the frequency content of the object increases beyond this point, coherence effects will become increasingly prominent. The class of objects for which an instrument can be considered to operate incoherently can thus be determined with this nomograph. Use of the nomograph will become clearer as we consider its application to various instruments.

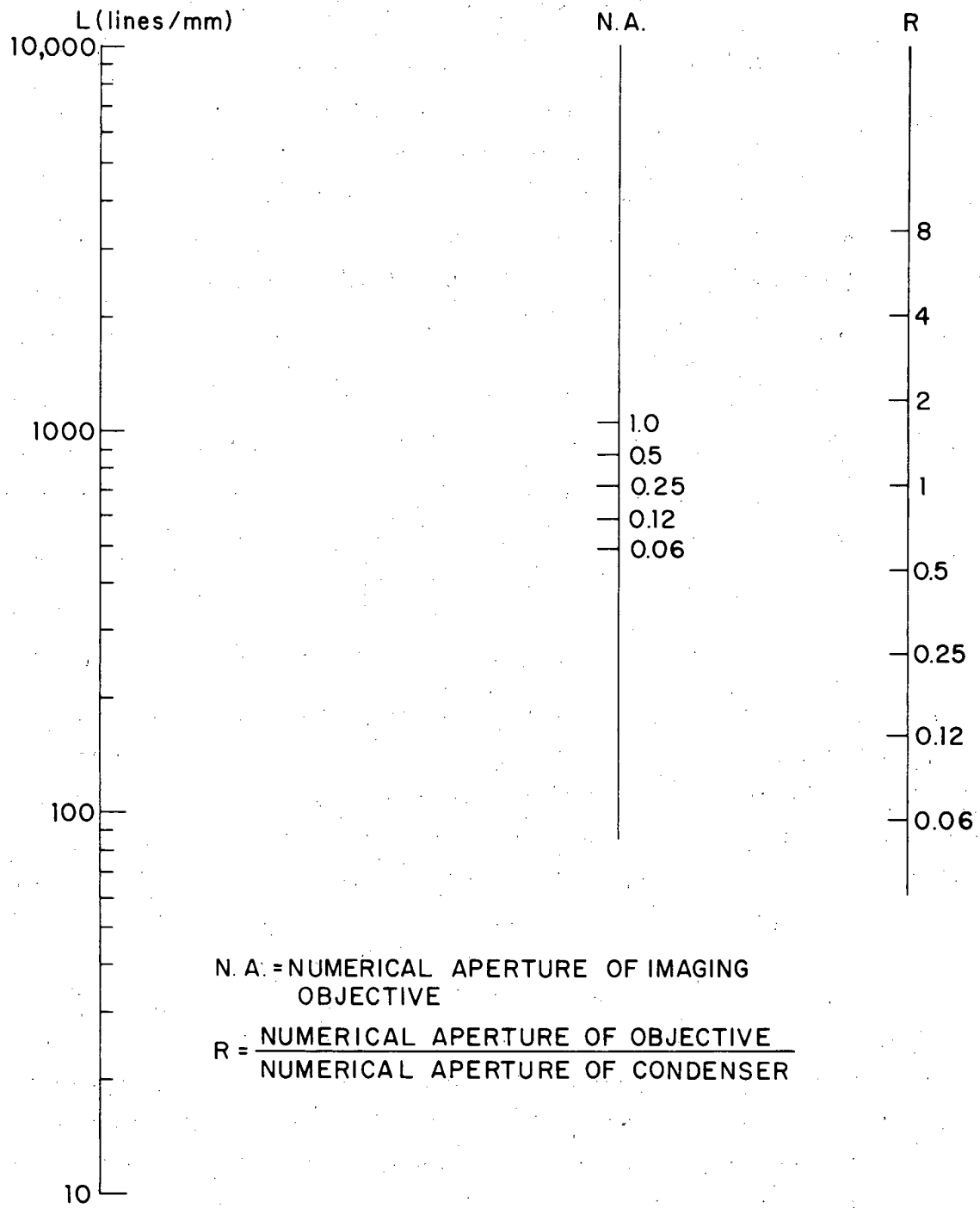

N. A. = NUMERICAL APERTURE OF IMAGING OBJECTIVE

$$R = \frac{\text{NUMERICAL APERTURE OF OBJECTIVE}}{\text{NUMERICAL APERTURE OF CONDENSER}}$$

Figure 1. Nomograph for Finding Conditions Under Which Coherence Effects Are Present in an Imaging System

APPLICATION OF NOMOGRAPH TO INSTRUMENTS IN CURRENT USE

Zoom 70 Microscope — This instrument employs light-table illumination for which the numerical aperture is 1.0. The numerical aperture of the imaging optics is approximately 0.05. Thus, R is 0.05 and N.A. is 0.05. As determined from the nomograph, the intercept frequency is about 10,000 ℓ/mm, which is far beyond the resolution limit of this or any other optical microscope. This microscope is therefore incoherent for all objects that can be examined optically.

High-Power Stereoviewer Microscope — This instrument employs condenser illumination; the numerical aperture of the illumination is adjustable from a minimum of 0.02 to a maximum of 0.40. As normally used, the illumination is set for its maximum numerical aperture. The three objectives usually used have numerical apertures of 0.10, 0.20, and 0.25. The intercept frequencies, as determined from the nomograph, are 2100 ℓ/mm, 1600 ℓ/mm, and 1400 ℓ/mm respectively for these three objectives when the condenser is wide open. In viewing photographic material in which the spatial frequencies are limited to values far below these frequencies, there will be no coherence effects. For objects such as resolution targets or biological specimens, coherence effects may be present particularly with the N.A. 0.20 and 0.25 objectives. If the condenser is stopped down to its minimum numerical aperture of 0.02, the intercept frequencies are about 20 ℓ/mm for all three objectives. In this case, the instrument is highly coherent for high-resolution photographic imagery, which means that the Stereoviewer can be used as a coherent spatial filtering system. This is in fact being done in a similar instrument in the grain filtering experiments to be discussed later.

Joyce-Loebl Microdensitometer — This instrument accepts standard microscope objectives for both condenser and objective. It is normally used with a condenser and objective of equal numerical apertures; thus R should always equal 1. A typical N.A. is 0.25. The intercept frequency is then 700 ℓ/mm. This microdensitometer will therefore show coherence effects for a wider class of objects than the Stereoviewer, although it may still be considered to be incoherent when tracing certain photographic records. It should be noted that a photographic object can have associated with it grain frequencies that are higher than those associated with the signal, and if the

scanning slit in the microdensitometer is small enough so that grain noise is prevalent, coherence effects may be present. If, however, the trace is made with a slit that is wide enough to smooth out the grain noise, coherence effects will be absent. This example points out the necessity for looking closely at the nature of the object and the operation of the instrument to determine if coherence effects are present.

Mann Microanalyzer — Since this instrument employs both a condenser and objective of N.A. 0.25, the discussion of the Joyce-Loebl microdensitometer applies here also.

Image Quantizer — This instrument also employs a condenser and objective of N.A. 0.25, and therefore the intercept frequency is also 700 ℓ/mm. This instrument is designed to operate on objects having a maximum frequency of about 5 ℓ/mm, and any higher frequencies will not be resolved by the printout. The Image Quantizer is thus incoherent for the class of objects for which it was designed to be used.

Projection Printer — This instrument contains objectives of numerical apertures 0.08, 0.16, 0.22, and 0.45, and condensers of numerical apertures 0.16, 0.30, and 0.45. Since each objective is supposed to be used in conjunction with the condenser most closely matched in N.A., the resulting values of R are between 0.5 and 1.0. Assuming the condensers and objectives are matched in this way, we find from the nomograph that the intercept frequencies for the four objectives are 800 ℓ/mm, 500 ℓ/mm, 800 ℓ/mm, and 1200 ℓ/mm, in order of increasing numerical aperture. Again, these frequencies are sufficiently high that the signal frequencies in photographic records will not be affected by coherence. Examination of photomicrographs of photographic targets made with this instrument under conditions where individual grains are resolved reveals that the images of the individual grains exhibit coherence effects, which is to be expected because the grains have higher frequencies associated with them than the intercept frequencies. When such a photomicrograph is scanned in the Image Quantizer, however, the optimum scanning aperture smears out the individual grain images, so that coherence will have no effect on the final trace.

This discussion of the individual instruments is summarized in Table 1. We can conclude that no coherence problems exist when these instruments are used for the normal examination of photographic material. This is basically due to the limited

TABLE 1

SUMMARY OF COHERENCE EFFECTS IN INSTRUMENTS CURRENTLY USED

Instrument	Condenser N.A.	Objective N.A.	Intercept Frequency* (ℓ/mm)	Comments
Zoom 70 Microscope	1.0	0.05	10,000	Incoherent under all conditions
High-Power Stereoviewer Microscope	0.40 as normally used. Can be stopped down to as low as 0.02.	0.10 0.20 0.25	2100 1600 1400	Intercept frequencies given assume that condenser N.A. = 0.40. They will decrease as the condenser is stopped down. Can become sufficiently coherent to do coherent spatial filtering if stopped down completely.
Joyce-Loebl Microdensitometer	Interchangeable. Normally equal to that of objective.	Accepts all standard microscope objectives. Typical value is 0.25.	700 for condenser and objective both of N.A. 0.25.	Intercept frequencies can be found from nomograph for other combinations of condenser and objective. Coherence effects may be expected in tracing photographic material if grain is not smoothed out by scanning aperture.
Mann Microanalyzer	0.25	0.25	700	Similar to Joyce-Loebl where coherence effects are concerned.
Image Quantizer	0.25	0.25	700	No coherence effects because resolution is far below intercept frequency.
Projection Printer	0.16 0.30 0.45	0.08 0.16 0.22 0.45	800 500 800 1200	These frequencies assume that objectives are properly matched to condensers. Coherence effects observable in images of grain, but generally averaged out by Image Quantizer scanning aperture.

*The intercept frequency is found from the nomograph in Figure 1. It represents the maximum spatial frequency an object can contain to ensure that coherence effects will not be present in a particular instrument.

spatial frequency content of the information of interest in such material and to the relatively low degree of coherence of the illumination. The coherence effects that may occur are generally associated with the grain noise in the film; such effects are of little importance in situations in which the grain noise is averaged out such as in microscopes where the magnification is insufficient to allow the individual grains to be detected or in scanning instruments where the grain noise is integrated out with a sufficiently large scanning aperture.

In situations in which coherence effects appear to be present, no simplified explanation can be made. The basic difficulty here is that the intensity distribution in the image is no longer linearly related to that of the object. This is not a severe problem when the image is to be observed visually. Where precise measurements of the intensity distribution in an image are required, however, as is often the case in techniques used for instrument evaluation, large errors can result. It is particularly in such cases that the possibility of the presence of coherence effects must be carefully considered.

CHAPTER 3

SHADED APERTURE STUDIES

WIENER FILTERS FOR THE IDT

The general purpose of this part of the program is to devise methods to minimize the loss of resolution in photographic images caused by the granular nature of the recording material. The specific analytical instrument of interest is the IDT, but many of the results obtained are directly applicable to the work being done on microscopes under other parts of the program.

Essentially, the IDT extracts information from the photograph by a scanning operation. A finite size scanning aperture must be used to scan across the film. Too large a scanning aperture causes a loss of resolution and too small a scanning aperture discloses the granular structure of the image, which again causes a loss of resolution.

In the past choosing the best size for the scanning aperture has been a matter of guesswork, and the aperture selected has always been a clear one. A clear aperture transmits completely all the light that passes through it, and blocks completely all the light outside its edges. Clear scanning apertures that are circular and rectangular are most commonly used.

In our present work we are primarily using "shaded" apertures. This means that the transmittance of the aperture at each point within its opening can be smoothly varying between zero and unity. The shape of the function showing the transmittance versus position within the scanning aperture is to be determined so that the scanning aperture is the "optimum" aperture. This will depend, of course, on our criterion for optimality, on the nature of the objects and grain structure, and on the type of exploitation tasks for which the scanning operation of the IDT is to be employed.

TYPES OF EXPLOITATION TASKS

The types of exploitation task that the IDT is to perform on the photographic material will have a profound influence on the form of the optimum filter. If, for example, the primary task was to locate sharp edges in the scene, a filter that takes the derivative of the scene energy distribution would be selected.

In general, however, many exploitation tasks are best served when the image of the scene has the highest fidelity possible. Here, fidelity means similarity between the distribution of luminance on the ground and the distribution of illuminance or energy levels in the photographic transparency. The scale of gray levels and the geometrical relationships in the original scene are then maintained. On the small scale, this maintenance of gray levels and geometrical relationships is difficult because of the granular structure of the recording material. For this type of exploitation task, therefore, the optimum filter will smooth the granular variations in transmittance of the transparency in such a way that the maximum fidelity is attained between the output of the IDT and the original scene.

This criterion of maximum fidelity can be given a simple mathematical expression. We define the "fidelity" as

$$F = 1 - D \ ,$$

where D is called the "fidelity defect" and is given by

$$D = \overline{\left(f_a - f_d\right)^2} \ ,$$

where f_a is the scan's actual output and f_d is its desired output. This definition states that the fidelity defect is the mean square difference between the actual output f_a of the scan and the desired output f_d. In our case, the desired output of the scan is simply the original scene that was imaged onto the grainy photographic material.

We are using this criterion of maximum fidelity F in designing our shaded scanning apertures or, as more often referred to, filters. Filters designed using the criterion of maximum fidelity F are called Wiener filters.

Thus, the type of exploitation tasks for which the present Wiener filters are best suited are those in which the analyst desires the most accurate rendition of the ground luminance levels and ground geometry. The present filters are designed to provide, to the maximum extent possible, this accurate rendition by smoothing the granular fluctuations in the photographic material.

Although we have considered the most important type of exploitation task here, it should be stressed that other types such as enhancing the edge detail at the cost of distorting the luminance levels (and possibly the geometry) would require another type of filter.

CLASSES OF OBJECTS AND FILMS

The optimum shaded aperture is designed to work well with a particular class of objects and films. The design of the particular aperture used depends on certain measured statistical properties of the film granularity and also on the statistical properties of the objects.

If we make a long trace across a uniformly exposed and processed sample of a particular photographic film such as 8430, we find that the transmittance of the film fluctuates. When a graph is made showing the number of times a particular transmittance value occurs versus the transmittance, a histogram of probability distribution of the transmittance is obtained. The height of the curve at any particular transmittance value indicates the relative probability of obtaining that value in any trace. The curve is characteristic of that film and exposure level (and also, perhaps, of the processing conditions).

Communications engineers working with Wiener filters for electrical signals have found that such filters work best when the noise (in our case, the grain) has a probability distribution of a particular shape. This shape is described by the function

$$P(T) = \frac{1}{\sigma\sqrt{2\pi}} e^{-(T-\bar{T})^2/2\sigma^2} ,$$

where P(T) is the probability density for getting a particular transmittance T. Here $\bar{T}$ is the average transmittance and σ^2 is the mean square transmittance, i.e., $\sigma^2 = \overline{T^2}$. This curve has the form shown in Figure 2. In the same figure we show the curve that has been found experimentally from measurements made on 8430 film. Examination of the figure shows that the two curves are similar, which means that the granularity of 8430 is of the type most suited to Wiener filtering.

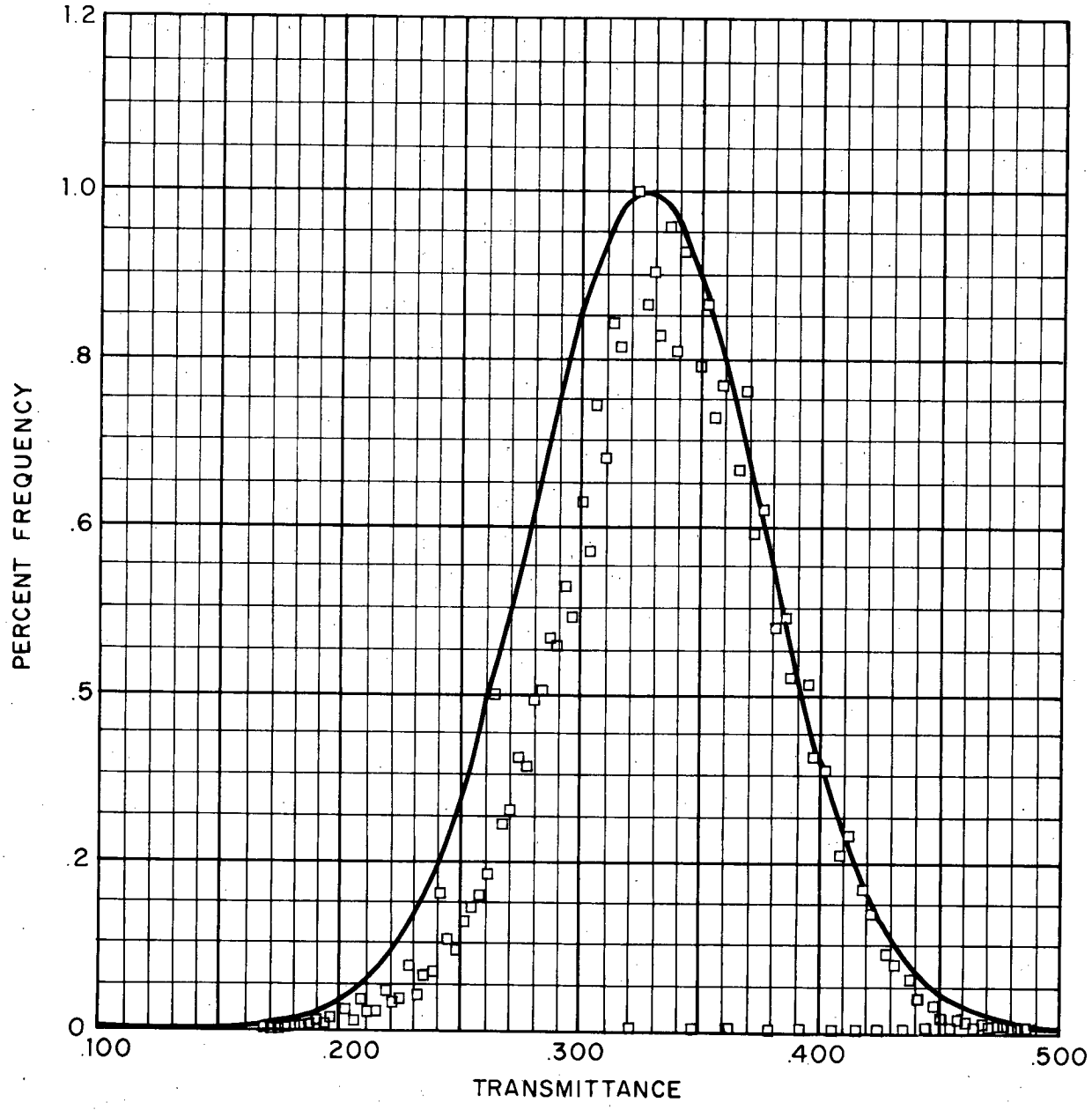

Figure 2. Measured Points of P(T) from Granularity Trace of 8430 Film Compared with Graph of $P(T) = \frac{1}{\sigma\sqrt{2\pi}} e^{-(T-\bar{T})^2/2\sigma^2}$

This form of transmittance probability distribution is most suited to Wiener filtering because the fidelity criterion F was chosen. The mean square difference D between the actual output f_a and the desired output f_d will be least when these outputs are equal. This condition will hold whenever the mean transmittance occurs, since it is identical with the actual scene level. For the P(T) given above, the mean value also happens to be the most probable value. Thus, the mean value and the most probable value of transmittance coincide, which a most satisfactory result. The maximum fidelity is then obtained when the most probable transmittance occurs. In cases of granular structures where the mean value and most probable value of transmittance do not coincide, the value that maximizes the fidelity is not the one that is most likely to occur. This situation would be unsatisfactory.

A similar situation is desirable for the distribution of transmittance levels in a typical scene. These levels should also have a distribution of the form P(T) shown in the equation above. By using a large scanning aperture to eliminate any grain effects, we have made traces of typical aerial scenes. The results are shown in Figure 3. The distribution in this case is not quite that desired (compare with shape of theoretical curve in Figure 2) but is close enough so that it should not be worrisome.

In summary, we can say that the classes of objects and films that have been found to be suitable for Wiener filtering are the general class of aerial scenes and the silver halide photographic recording materials that are in current use. Fortunately, our method of processing is well suited to the nature of the objects and films of interest.

EXPECTED IMPROVEMENTS IN IDT TRACES

During last year's program the shaded apertures were based on an approximation to the actual optimum filter. Results obtained with these apertures and with microsector targets were shown in the final report on that program. The traces appeared to be improved in resolution, rendering of straight lines, and maintenance of geometrical shapes. Since that time, however, refinements have been incorporated into the methods used for determining the optimum shaded apertures, and correspondingly better results are expected. Improvements in the technique include a more accurate estimate of the effect of the taking lens and film on the shape of the optimum aperture (see Appendix A). Although the new apertures have not yet been constructed and used

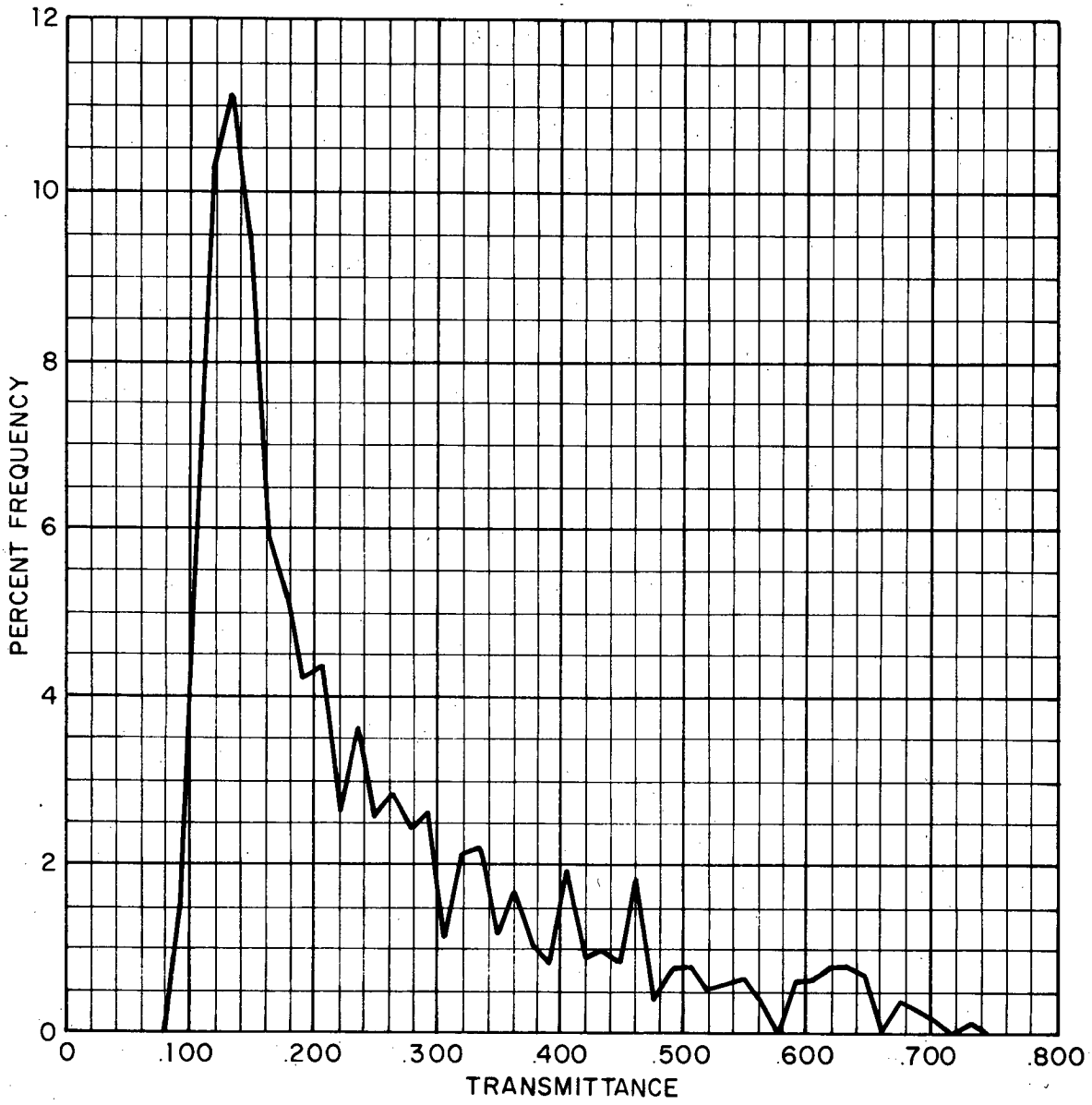

Figure 3. Distribution of Transmittance Levels in a Typical Photographic Scene

in IDT experiments, we feel that they will be an important factor in obtaining better traces.

Filters that approximate the form of the Wiener filters employed last year have been used in the microscope filtering work described later in this chapter. The results obtained in that work show an increased contrast and a beneficial smoothing of the grain noise. These results are encouraging because similar, although not identical, types of filtering will be used in the IDT in this part of the program.

In summary, the prospects for the improvement of IDT traces by using the shaded apertures seem very good. This expectation is based on last year's results, on the results obtained this year with the microscope filtering, and on a realization that the method of design of the filters to be used in this year's work is significantly improved over previous methods. Further quantitative bases for determining the improvement must await experimental work, which is just beginning at this time.

CURRENT MODIFICATIONS IN COMPUTER PROGRAM

Several improvements that are more than just changes in computation methods have been made in the computer program that processes the film granularity data and designs the optimum shaded apertures. These are described below.

In the work performed during last year's program, we assumed that the desired signal or object to be recovered by processing was the object as it existed on the film, apart from granularity limitations. That is, we assumed that the scene of interest was the scene image after it had passed through the lens and film of the taking system. Although this assumption is a good working hypothesis in some cases, it is not as suited to real world situations as it is to laboratory experiments.

In operational situations, since we want to recover the original scene, we would expect to have to account for the degradations imposed on the scene image by the finite resolution of the taking lens and film. These degradations are represented by the transfer functions of lens and film in the taking system. Appendix A gives a complete analysis of the effect of the finite resolution of the taking system.

During last year's work we found that the optimum shaded aperture determined by the computer had some negative transmittance regions. Negative intensity transmittance is of course unrealizable. Therefore, we have made another improvement by

approximating the form of the optimum shaded aperture by a close-to-optimum realizable shaded aperture. To determine how close the aperture is to optimum, we have now included in the computer program a calculation of the mean square error obtained with the two filters. As previously explained, the mean square error is the error between the actual output trace and the desired output trace. This should provide us with a quantitative basis for determining the best approximation to the optimum. Calculation will in some cases be much faster than constructing and trying several approximate shaded apertures. For a derivation of the form of this mean square error, see Appendix B.

GRAIN NOISE FILTERING IN THE MICROSCOPE

The theory of Wiener filtering to minimize grain noise from photographic film can just as easily be applied to the microscope or any other optical instrument as to a microdensitometer. To study the feasibility of using Wiener filters in the microscope for high resolution photointerpretation, some experiments were first performed using a low-resolution, grainy film (Tri-X) and approximations to a Wiener filter, rather than an actual computer-generated Wiener filter. In the microscope, the Wiener filter (or, more appropriately, the grain-noise filter) can most suitably be placed at the image of the source located just above the objective lens (in a coherent system, this would be the Fourier transform plane). A Wild condenser-illuminated microscope was used with a 10X Wild objective (0.45 N.A.) and a 10X eyepiece. The position and size of the transform plane vary according to the position of the condenser lens. For this preliminary study, the condenser was adjusted to its lowest position with the iris diaphragm stopped down, corresponding to the most coherent case and having the most well defined transform. In this position, the transform plane was located just within the barrel of the objective lens where a filter could be conveniently placed and held with a retaining ring.

The filters used in this feasibility study were made by recording a defocused image of a black disk of the appropriate size on Recordak AHU microfilm. The transform plane dimensions were determined by placing a ruling of approximately 100 ℓ/mm on the object stage and then exposing a piece of film in the transform plane. A measurement of the order separation made it easy to determine the approximate diameter

of the filter to be used. Figure 4 is a microdensitometer trace of one of the filters used. The size and shape of the filter could easily be changed by varying the magnification and the amount of defocusing in the imaging system used to make the filters. A number of filters were tried, and the filter represented in Figure 4 seemed to give the best results. No real effort has yet been made to optimize the shape of the filter; this will not be done until we have obtained results for 8430 film.

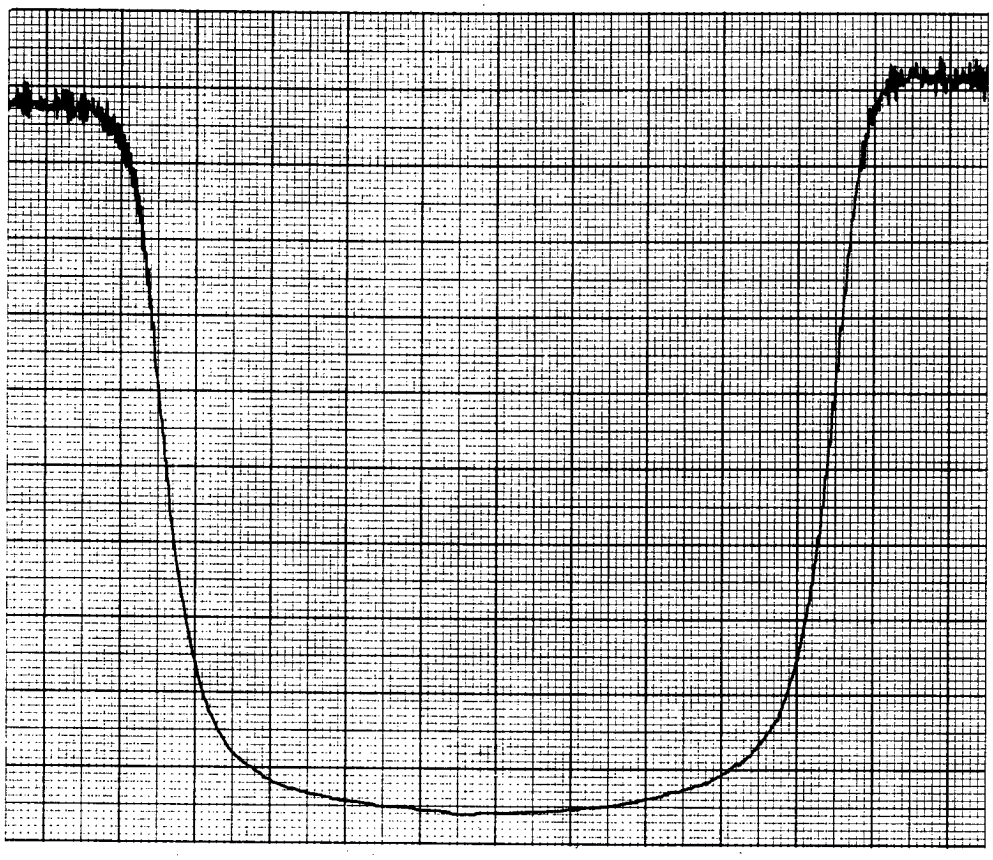

Figure 4. Microdensitometer Trace of the Grain-Noise Filter Used in the Experiments with Tri-X Film (100X magnification)

Two targets were used for this initial study of Tri-X film, an Air Force three-bar resolution target and a circularly symmetric converging sector target. The three-bar target was contact-printed, and the sector target was projection-printed onto Tri-X film developed in D-76 to provide grain-limited images of 60 to 80 ℓ/mm that are clearly visible with the 10X objective and 10X eyepiece.

For visual comparison of the effects of filtering, two similar 10X Wild objectives were used, one with and one without a filter. The filter was placed in the objective lens and visually aligned with the image of the source when the objective was in its operating position. Once a filter was found that showed visual improvement, photomicrographs were made to provide a better comparison. Figure 5a shows a three-bar target on Tri-X film as seen with an unfiltered 10X objective. Figure 5b shows the same grain-limited image viewed with an objective containing the filter as shown in Figure 4. It can easily be seen that the signal contrast improved and that edges are smoother and better defined. Though there is no apparent increase in resolution in this example, it is possible that the contrast increase could make an additional resolution element visible, thereby giving an apparent resolution increase. Figure 6 shows the same filtering for the circularly symmetric sector target; again the contrast has been increased and the edges smoothed and sharpened.

These results demonstrate the feasibility of using Wiener filters in a microscope. In the experiments with Tri-X, the filters were designed to be compatible with the resolution capabilities of Tri-X. To make these filters suitable for use with 8430 film, it is merely necessary to scale them to the proper size. An initial experiment has been performed using as an object a microdot resolution target contact-printed onto 8430. The three-bar resolution on the contact print is 200 ℓ/mm. Figure 7 shows photomicrographs of both the filtered and unfiltered image. There seemed to be some improvement in the filtered image, although it is not apparent in the photographic reproduction. Since this initial work is promising, future work will be aimed at optimizing the size and shape of the filter by using the results of the Wiener filter studies for the IDT, which apply to 8430 film.

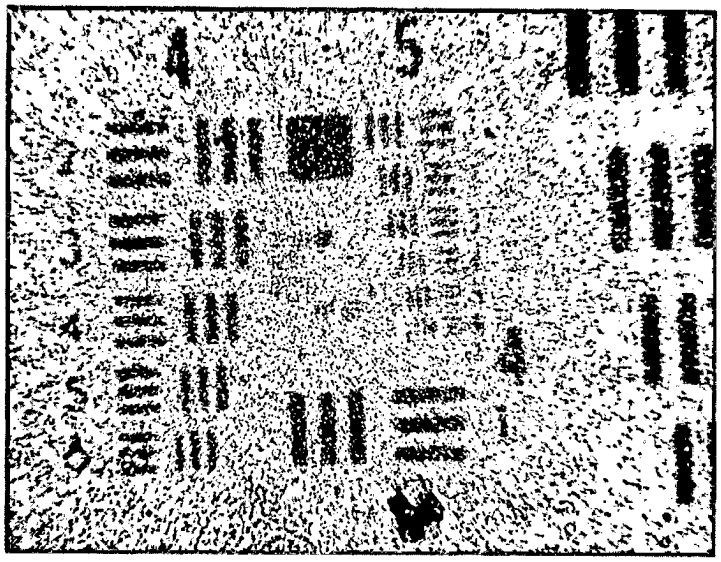

a. Unfiltered

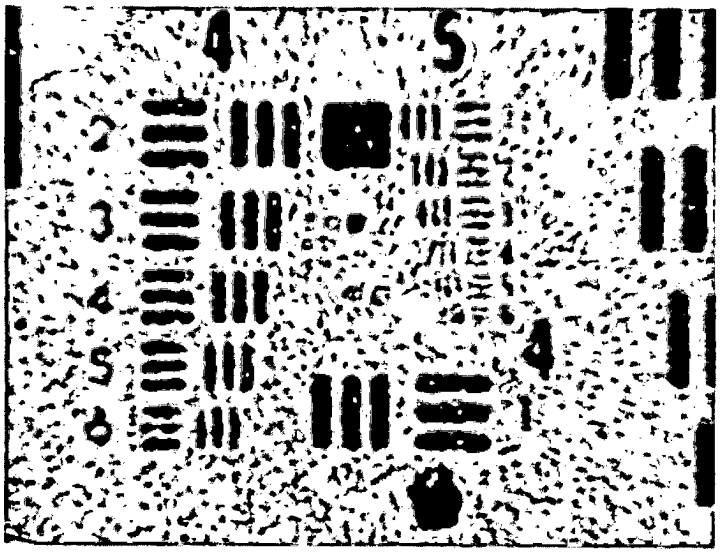

b. With Grain-Noise Filter

Figure 5. Photomicrographs of Three-Bar Target Image on Tri-X Film

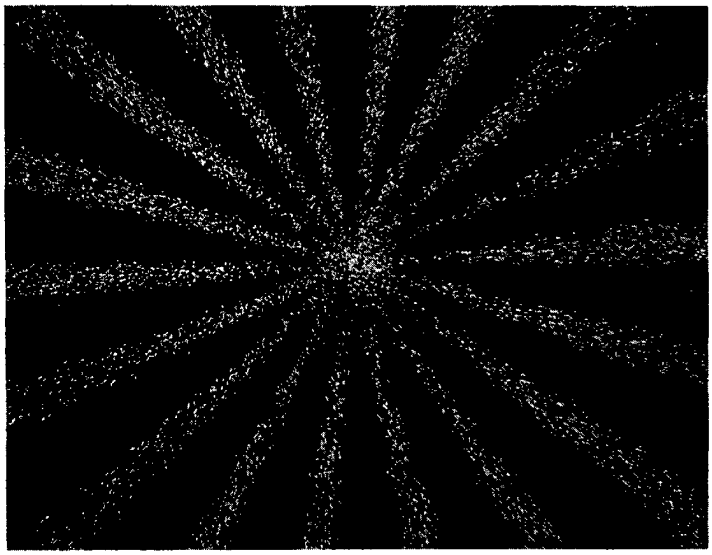

a. Unfiltered

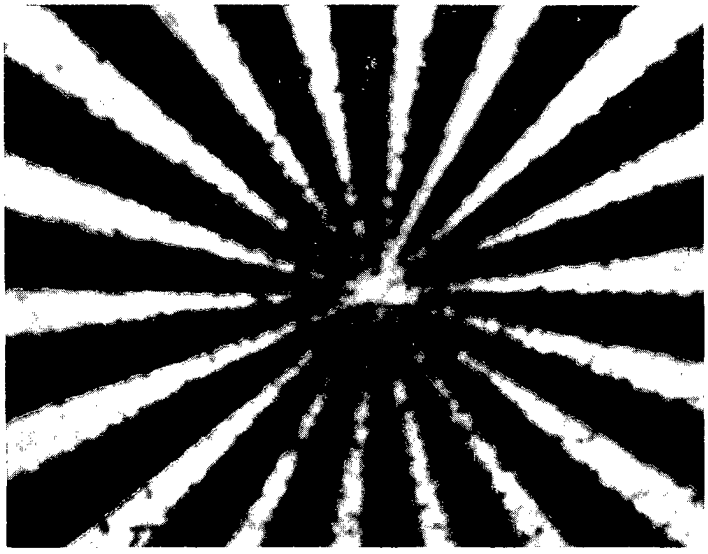

b. With Grain-Noise Filter

Figure 6. Photomicrographs of Sector Target on Tri-X Film

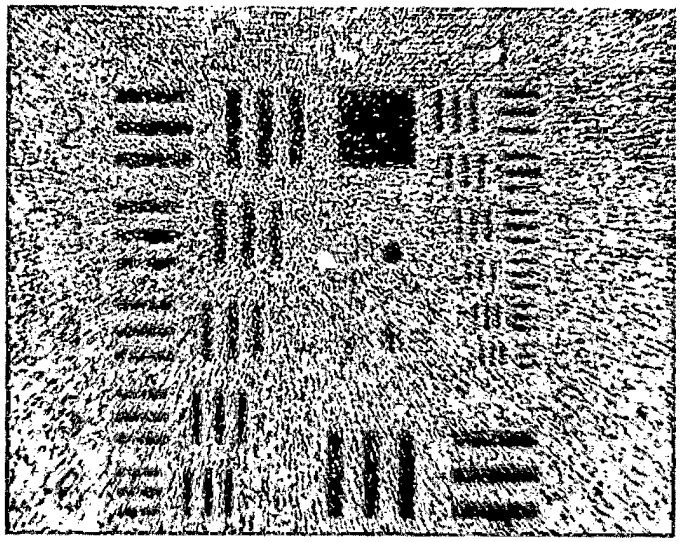

a. Unfiltered

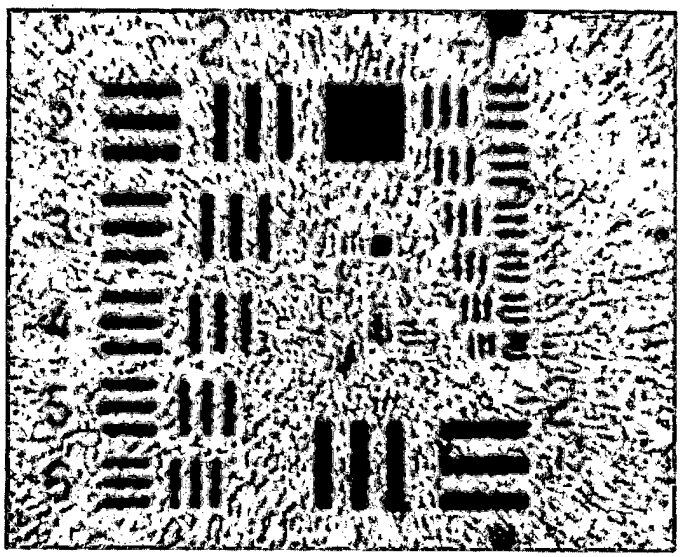

b. With Grain-Noise Filter

Figure 7. Photomicrographs of Three-Bar Target Image on 8430 Film

COLOR FILTERS FOR MICROSCOPES

The object of this phase of the contract is to determine if a microscope can be operated in such a way that information in different frequency bands is imaged in different colors and, if so, to see whether such a situation would be advantageous in viewing photographic imagery. Two types of microscopes were considered — the Zoom 70 (employing light-table illumination) and the High-Power Stereoviewer (employing condenser illumination). Because the approach is basically different for these two instruments, they will be discussed separately.

HIGH-POWER STEREOVIEWER

It is well known that bandpass filtering can be accomplished in a coherent optical system since each circle in the filter plane represents a single frequency of the amplitude transmittance of the object. One possible way of performing color filtering in the Stereoviewer would be to stop down the condenser aperture as far as possible, thus approximating coherent illumination very closely, and to use annular filters of various colors in the back focal plane of the imaging objective. A specific range of frequencies corresponding to the passband of a particular annulus would then be imaged in the color transmitted by that annulus. The main drawback to this method is that highly coherent light must be used. Any advantage to be gained would probably be more than offset by the coherence effects that would be present.

Another method that has been examined appears to combine the desirable effects of the method described above while utilizing light with a very low degree of coherence. This method is based on the technique of dark-field illumination, the basic idea of which is shown in Figure 8. The stop placed in the condenser absorbs the cone of illumination that would normally fill the aperture of the objective but passes an annular cone of rays that fall outside the objective. If no object is in place, a completely dark field is seen upon viewing through the microscope. If, however, an object is in place, some light from the annular cone will be diffracted by details in the object and will enter the objective and contribute toward forming an image. Light diffracted from the object representing all spatial frequencies from the normal cutoff frequency of the objective down to, but not including, zero, will enter the objective and contribute to the image. Zero spatial frequency is not included so that clear

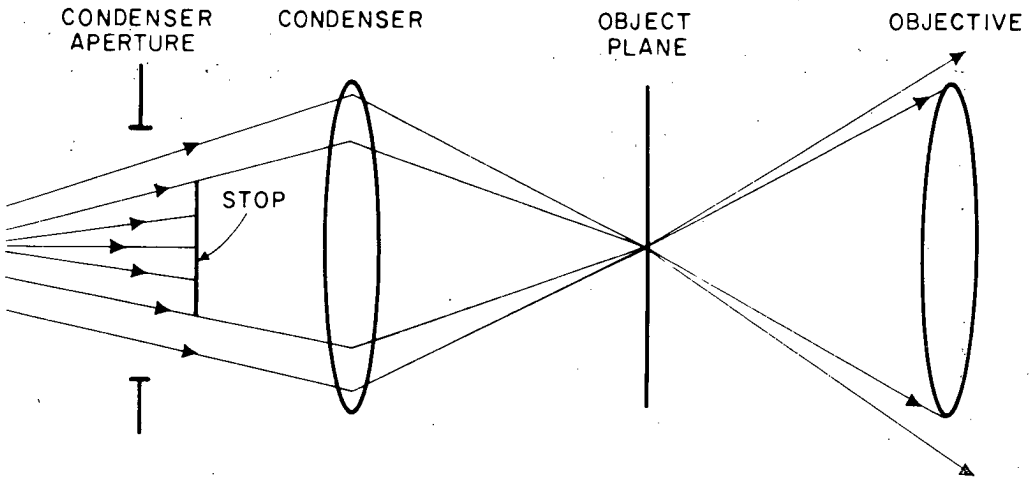

Figure 8. Optical System of Dark-Field Illumination in a Microscope

areas will image as dark. The total image thus appears as bright images of the details in the object superimposed on a dark background. If we consider an object consisting of both fine and coarse opaque details on a clear background, then under dark-field illumination, the fine details and the edges of the coarse details will appear bright and the clear background and the central parts of the coarse details will be dark. Thus, for the fine opaque details, the normal appearance of dark details on a bright background is reversed, while for the coarse details, the edges appear bright against a dark background.

In our experiments, we have used a filter in the condenser aperture consisting of a central circle that transmits green light and an outer annulus that transmits red. The size of the green circle corresponds to the size of the stop in Figure 8. The illumination might thus be said to consist of a combination of green bright-field illumination and red dark-field illumination. An object consisting of fine opaque details on a clear background should then image as red details on a green background. Figure 9 shows photomicrographs of a section of lens tissue that illustrate this effect. Although the background in the color print has yellowed in the reproduction process, visually it appears bright green. Also, some of the fine details evident upon direct viewing through the microscope are lost in the photographic reproduction, but it definitely appears that some features, particularly in the finest structures visible, become more prominent and easily seen under two-color illumination than under normal illumination. The two-color illumination provides an additional advantage in that the effective visual contrast can be varied by

a. Two-Color Illumination

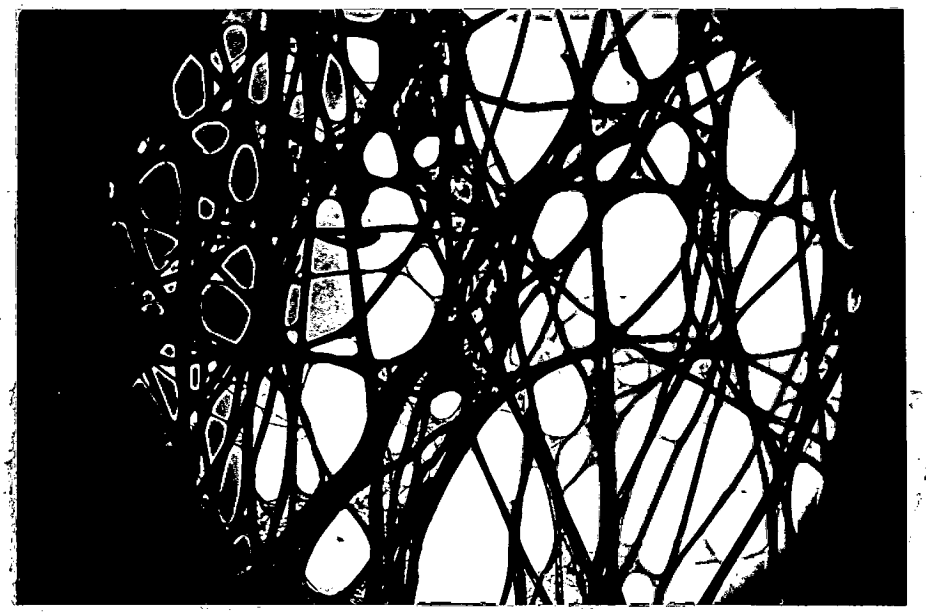

b. Normal White-Light Illumination

Figure 9. Photomicrographs of a Section of Lens Tissue

varying the ratio of red to green light forming the image. This can be done by varying the size of the iris diaphragm in the condenser aperture. If this iris is set at just the size of the green circle, only green light forms the image. Red light appears as the iris is opened and its amount increases as the iris is opened wider. An observer can thus select the contrast that appears optimum to him for viewing any particular detail.

Although this type of illumination does not produce bandpass filtering in any sense, it does cause a type of enhancement of fine detail that produces the primary effect we would hope to achieve with bandpass filtering. Though very dramatic effects can be achieved with certain objects, results obtained to date with photographic objects are not nearly so pronounced, primarily because of the grain and the gray scale associated with the photographic image. Even a uniform area of a photograph has high frequencies associated with it caused by graininess of the image; such an area will therefore not consist exclusively of a green image under this type of illumination, but will have some red mixed in. In addition, the image consists of levels of transmission rather than opaque details, which means that this mixing of red and green will occur over the entire image. There is thus simply a tendency for the two colors to blend together over the entire field and, to date, no apparent enhancement of details in photographic images has been observed. As this is a fundamental limitation imposed by the nature of photographic objects, we conclude that this is not a useful approach to enhance the viewing of photographic material.

ZOOM 70 MICROSCOPE

Since this instrument employs a light-table illuminator, no control of the illumination is possible. We have already shown that this instrument can be considered incoherent. Even though this allows no flexibility in its use for filtering, as does the Stereoviewer, it allows a linear systems analysis to be performed. It is well known that for an incoherent imaging system the transfer function is the autoconvolution of the pupil function of the imaging lens. Again, the filter we have considered consists of a central green circle and an outer red annulus. In this case, the filter is placed in the pupil of the objective. We can then find separate transfer functions for red and green light, and the imaging characteristics can be inferred from examining these two transfer functions.

As an example, Figure 10 shows the two transfer functions that result if the central green circle is half the pupil diameter, assuming that there are no phase aberrations in the imaging system. Although the green aperture diameter is half that of the total aperture, the cutoff frequency for the green transfer function is somewhat more than half that of the red transfer function because of the shorter wavelength of the green light. The salient features shown by Figure 10 are that a range of high frequencies image exclusively in red and the low frequencies image in a mixture of red and green. The modulation of high frequencies that image in red is, however, significantly attenuated. In addition, the low frequencies also image in red as well as in green, so there will be less color contrast in the image than if the low and high frequencies imaged in different colors. We saw that it was possible with the Stereoviewer to control the color contrast in the image by adjusting the condenser aperture. This possibility is not available in the Zoom 70 because increasing the proportion of

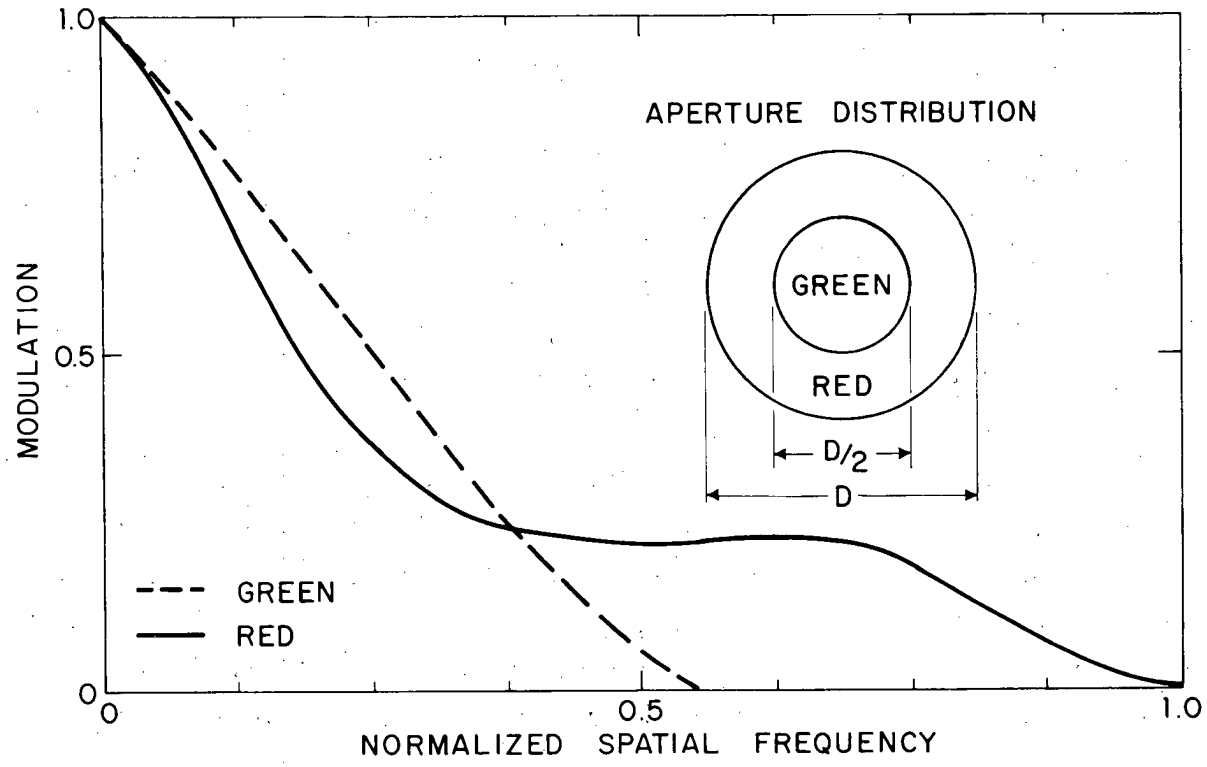

Figure 10. Two-Color Transfer Functions for the Zoom 70 When the Pupil Distribution is the Aperture Shown

red light in the image by increasing the density of the green filter would increase the proportion of red in not only the high frequencies but also in the low frequencies.

It thus appears that the effects obtainable with this instrument should be less pronounced than those obtained with the Stereoviewer, and experiments confirm this. When this type of filter is used with the Zoom 70 microscope to view a target similar to that shown in Figure 9, no significant color contrast is observed, but merely an image consisting of a uniform mixture of the two colors. The image is noticeably poorer than that obtained without the filter.

It is clear that the Stereoviewer is a far more promising instrument for this type of work than the Zoom 70. It is probably possible to obtain some sort of effect with the Zoom 70 by optimizing the filter configuration, but it does not appear that this is a useful approach, particularly since any effect would be lessened when a photographic object is viewed.

SPATIAL FILTERING IN SCANNING SYSTEMS

During this quarter some effort was expended obtaining equipment to use in performing scanning system filtering experiments. It was decided that the initial feasibility could be shown with a one-dimensional system such as the microdensitometer. We will modify the microdensitometer by using a laser source and perform our filtering by placing masks in the filter plane of the system. This will enable us to show feasibility of the idea with the simplest conceivable system. We will print our answers out on recording paper with a pen readout and not try to print out gray scale imagery, which may be done at a future date if desired. Once feasibility is shown, we will then investigate use of a standard illumination system for the filtering experiments.

Initially, a halftone removal experiment will be performed. A continuous density wedge (a ramp function) will be photographed through a low pass system and rastered such that the sampling theorem is obeyed. The rastered object will be scanned and passed through an appropriate bandpass filter so that the raster does not appear on the output side of the system. The filter size will be picked in accordance with the sampling theorem and the system parameters. If this simple raster removal experiment is successful, then more complicated experiments such as differentiation, contrast enhancement, and high pass filtering will be attempted.

APPENDIXES

APPENDIX A

EFFECT OF TAKING SYSTEM RESOLUTION ON THE FORM OF THE OPTIMUM SHADED APERTURE

We can represent the physical transfer of the light distribution from ground scene to final IDT output trace as shown in Figure A-1. The lens-film combination of the taking system is represented by a transfer function $T(\omega)$, ω being a spatial frequency. This transfer function expresses the finite resolution of the taking system.

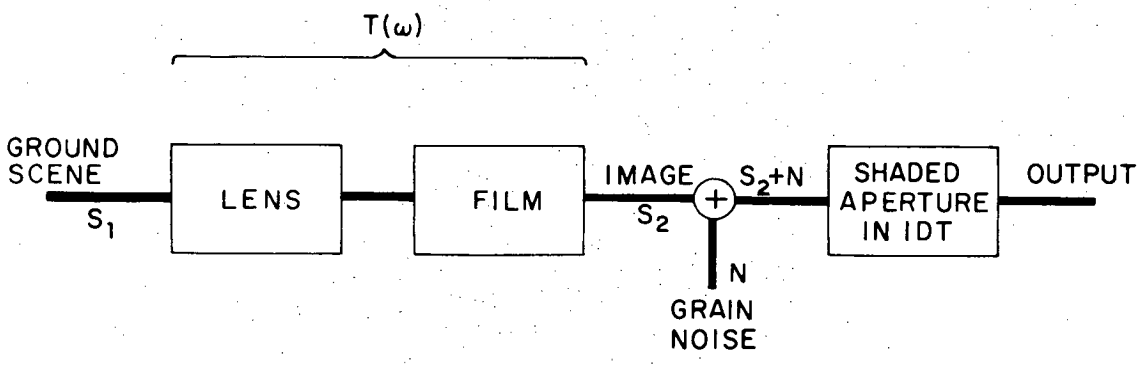

Figure A-1. Physical Transfer of Light Distribution from Ground Scene to Final IDT Output

The ground scene is represented as a signal S_1 and the image after diffusion through the film emulsion is represented by S_2. The grain noise N is then added to the signal S_2 to produce the developed grainy image $S_2 + N$. This is processed using the shaded aperture in the IDT.

We know that the general form at the optimum Wiener filter in frequency space is[1]

$$H(\omega) = \frac{\Phi_{id}(\omega)}{\Phi_{ii}(\omega)} \quad ,$$

where

$\Phi_{id}(\omega)$ = cross power spectrum of input i and desired output d of IDT

$\Phi_{ii}(\omega)$ = power spectrum of input to IDT .

1. Y.W. Lee, "Statistical Theory of Communication (New York, N.Y.: John Wiley & Sons, Inc., 1960). p. 370.

Now we use the knowledge that the input is

$$i = S_2 + N$$

and the desired signal is the original ground scene:

$$d = S_1 \quad .$$

Then the filter has the form

$$H(\omega) = \frac{\Phi_{S_2S_1}(\omega)}{\Phi_{S_2S_2}(\omega) + \Phi_{NN}(\omega)} \quad ,$$

where we have assumed as before that both the signals S_1 and S_2 are uncorrelated with the grain noise N.

Now it is known from Fourier analysis that

$$\Phi_{S_2S_1}(\omega) = \Phi_{S_1S_1}(\omega)\, T(\omega)$$

$$\Phi_{S_2S_2}(\omega) = \Phi_{S_1S_1}(\omega) |T(\omega)|^2 \quad ,$$

where

$$T(\omega) = T_{lens}(\omega) \cdot T_{film}(\omega) \quad .$$

Finally, we obtain the result showing the effect of the finite taking system resolution on the form of the Wiener filter:

$$H(\omega) = \frac{\Phi_{S_1S_1}(\omega)\, T(\omega)}{\Phi_{S_1S_1}(\omega) |T(\omega)|^2 + \Phi_{NN}(\omega)} \quad .$$

Of course, to get the actual shape of the shaded aperture transmission function, we must transform this $H(\omega)$ from frequency space back to distance space.

To show that this form is reasonable, consider the limiting case where there is no noise. Then $H(\omega)$ becomes

$$H(\omega) = \frac{1}{T(\omega)} \quad ;$$

that is, the shaded aperture acts as a simple inverse filter to compensate directly for the losses imposed on the image resolution by the taking system transfer function $T(\omega)$.

It is also useful to look at the case where the noise is small compared to the signal on the film. In this case we can expand the general expression for $H(\omega)$ given above to obtain

$$H(\omega) = \frac{1}{T(\omega)} \left[1 - \frac{\Phi_{NN}(\omega)}{\Phi_{S_2S_2}(\omega)} \right] .$$

Note that at any frequency ω, the ratio $\Phi_{S_2S_2} / \Phi_{NN}$ is the <u>received</u> signal-to-noise ratio. Thus, we see that the effect of noise on the inverse filtering operation represented by $H(\omega) = 1/T(\omega)$ is to pass less of the image through the shaded aperture at those frequencies where the <u>received</u> signal-to-noise ratio becomes smaller.

APPENDIX B

MEAN SQUARE ERROR

The mean square error between the actual output of the IDT and the desired output is a measure of the fidelity of the actual output to that desired. This error is called the fidelity defect and is represented by

$$D = \overline{\left[f_a(x) - f_d(x) \right]^2} \ ,$$

where the bar indicates an average. We can now expand this as

$$D = \overline{f_a^2(x)} + \overline{f_d^2(x)} - 2\overline{f_a(x)\, f_d(x)}$$

$$= \phi_{aa}(o) + \phi_{dd}(o) - 2\phi_{ad}(o) \ .$$

In this last form, we have just written the mean square quantities in their equivalent form as the zero ordinates of the correlation functions. We now use linear system theory to write

$$D = \int \Phi_{dd}(\omega) \frac{d\omega}{2\pi} + \int \Phi_{aa}(\omega) \frac{d\omega}{2\pi} - 2 \int \Phi_{ad}(\omega) \frac{d\omega}{2\pi} \ .$$

Using the diagram shown in Appendix A, we can rewrite this as

$$D = \int \Phi_{S_1S_1}(\omega) \frac{d\omega}{2\pi} + \int \left[\Phi_{S_2S_2}(\omega) + \Phi_{NN}(\omega) \right] |H(\omega)|^2 \frac{d\omega}{2\pi}$$

$$- 2 \int \Phi_{S_1S_1}(\omega)\, H(\omega) \frac{d\omega}{2\pi}$$

$$= \int \Phi_{S_1S_1}(\omega) \left[|T(\omega)\, H(\omega)|^2 - 2T(\omega)\, H(\omega) + 1 \right] \frac{d\omega}{2\pi}$$

$$+ \int \Phi_{NN}(\omega) |H(\omega)|^2 \frac{d\omega}{2\pi} \ .$$

The calculated error or fidelity defect D now depends on the power spectra of the original scene S_1 and noise N and on the transfer functions of the taking system's lens-film combination $T(\omega)$ and of the scanning system $H(\omega)$.

By calculating D for the clear scanning aperture, for the optimum shaded aperture, and for the approximately optimum shaded aperture, we can learn two things: first, how much improvement can be expected in using a shaded rather than clear aperture, and second, how closely the approximate realizable aperture approaches the optimum in performance.